

Article

Development of a Fuel Model for *Cistus* spp. and Testing Its Fire Behavior Prediction Performance

Miltiadis Athanasiou ^{1,*} , Aristotelis Martinis ² , Evangelia Korakaki ³  and Evangelia V. Avramidou ⁴ ¹ Wildfire Management Consulting and Training, 8 Thoma Paleologou St., 13673 Athens, Greece² Department of Environment, Ionian University, M. Minotou-Giannopoulou St., 29100 Zakynthos, Greece; amartinis@ionio.gr³ Laboratory of Tree Physiology, Institute of Mediterranean Forest Ecosystems, ELGO-DIMITRA, Terma Alkmanos, Ilisia, 11528 Athens, Greece; e.korakaki@fria.gr⁴ Laboratory of Forest Genetics and Biotechnology, Institute of Mediterranean Forest Ecosystems, ELGO-DIMITRA, Terma Alkmanos, Ilisia, 11528 Athens, Greece; avramidou@fria.gr

* Correspondence: info@m-athanasiou.gr

Abstract: This paper presents the development of a fuel model that can describe fuel situations in areas dominated by *Cistus* spp. (rockrose) in Greece. In order to obtain the necessary fuel data, thirty (30) 1 m² plots were destructively sampled in phryganic areas dominated by *Cistus creticus*, *Cistus parviflorus*, and *Cistus salvifolius* in western Greece. To develop the fuel model for *Cistus* spp., field measurements were supplemented with published parameter values for *Cistus salvifolius*. The resulting fuel model (with a height of 9.44 cm) is suitable for describing *Cistus* spp.-dominated phryganic areas of relatively low vegetation height in southeastern Europe. Once developed, the fuel model was inputted into the BehavePlus system to produce surface fire rate of spread predictions (ROS_{pred}, m·min⁻¹), which were then compared to 21 surface fire ROS field observations (ROS_{obs}) obtained from wildfires or prescribed burns in areas covered by *Cistus* spp. It was found that the ROS for the *Cistus* spp. fuel model significantly underpredicted the actual ROS. A statistically significant linear regression equation was developed to mathematically describe the relationship between the predicted and observed ROS. This equation can be used to adjust BehavePlus predictions to more accurately reflect the real-world fire behavior for this fuel type.

Keywords: fuel model; destructive fuel sampling; fire behavior prediction; *Cistus* spp.



Citation: Athanasiou, M.; Martinis, A.; Korakaki, E.; Avramidou, E.V.

Development of a Fuel Model for *Cistus* spp. and Testing Its Fire Behavior Prediction Performance.

Fire **2023**, *6*, 247. <https://doi.org/10.3390/fire6070247>

Academic Editor: Grant Williamson

Received: 29 April 2023

Revised: 15 June 2023

Accepted: 21 June 2023

Published: 25 June 2023



Copyright: © 2023 by the authors. Licensee MDPI, Basel, Switzerland. This article is an open access article distributed under the terms and conditions of the Creative Commons Attribution (CC BY) license (<https://creativecommons.org/licenses/by/4.0/>).

1. Introduction

Reliable forest fire behavior prediction and relatively accurate quantitative estimates of potential wildland fire rate of spread (ROS, m·min⁻¹) and flame length (L, m), which is the main visual manifestation [1] of fire line intensity (I, kW·m⁻¹) [2], support effective wildfire management. Predictions and estimates of ROS and L can either be based on the experience of fire practitioners and managers or on models included in software systems. Fire behavior models, the core of fire behavior prediction software systems, can be adopted in forest management, fire prevention, and suppression only if their degree of reliability, strengths, and weaknesses are well known [3].

The most popular and robust fire behavior model for predicting ROS in surface fuels globally is Rothermel's [4] mathematical model, mainly due to its good documentation, practicality, and significant number of studies that tested its prediction performance for various fuel types. Its strengths and weaknesses are quite well known [5,6] due to the extensive testing that has taken place (i) in the laboratory, (ii) in experimental field burns, and (iii) in actual wildfires of low to medium intensity [7–9] or of high intensity [10,11]. Rothermel's model is the core component of the BehavePlus fire behavior modeling system [12,13] and of various wildfire spread simulation systems [14] such as the two-dimensional deterministic fire growth model FARSITE [15–17], which is now included in the FlamMap system [17].

In the years that passed since the first publication of Rothermel's model, which has a semi-empirical basis, there have been numerous efforts to improve it [13,18]. It has received significant scrutiny and a number of improvements have been adopted in practice, as listed by Andrews [6]. While Rothermel's model maintained a prominent position in fire behavior modeling around the world, many other empirical modeling efforts have tried to improve simplicity [19–21] or achieve a better representation of local conditions [22–24]. Obviously, during this time, there have also been many efforts to develop more advanced physically based models [25–29], including models that take into consideration the interaction of fire with the atmosphere [30].

Examples of coupled atmosphere–fire models include CAWFE (Coupled Atmosphere–Wildland Fire Environment, [31]), two related models based on the WRF (Weather Research and Forecasting) atmospheric model, WRF-Fire [32] and WRF-SFire [33], and Meso-NH/ForeFire [34], which is a coupling of the non-hydrostatic mesoscale atmospheric model Meso-NH with a one-dimensional fire spread model ForeFire [35].

BehavePlus, although first launched as BEHAVE in 1984, is still widely used around the world, not only because it is well documented, tested, and free to use, but also because Rothermel's model requires fuel as an external input in the form of a fuel model. Thus, it can be applied anywhere in the world provided that an appropriate fuel description, a fuel model, is available. This makes BehavePlus a flexible, non-spatial system that provides a quick and easy way to assess potential fire behavior through its 'point-based' fire modeling approach.

From its first edition, the BEHAVE system facilitated the development of custom fuel models [36] that can be site specific. A fuel model is described as a set of average values of specific parameters that describe a particular type of vegetation in the form that is required to be used with Rothermel's model and, accordingly, with the BehavePlus system. Each such stylized fuel model consists of 11 average values [36,37].

The calculation of the surface fire rate of spread requires (i) a fuel model, (ii) midflame wind speed [38], (iii) slope (%), and (iv) fuel moisture content (FMC, %) [13]. In BehavePlus, midflame wind speed is the average wind speed from 1.5 to 3 ft above the ground [39]. It is the wind that affects surface fire spread and it is customary to describe it as the eye level wind speed. A user may specify values for midflame wind speed by either adjusting 6.1 m (20 ft) wind to midflame height or by skipping that step using a handheld anemometer. The wind speed at a 6.1 m (20 ft) height is either measured or estimated by reducing the 10 m height wind speed accordingly [39–42].

Dimitrakopoulos [43,44] developed several fuel models to describe Mediterranean fuel types in Greece. Later testing with fire behavior observations in real fires demonstrated that BehavePlus can be a useful tool for predictions of surface wildfire ROS in tall and short maquis, phryganic areas where the dominant species is *Sarcopoterium spinosum*, and grass [45].

Phryganic areas in Greece are covered by "phrygana", a vegetation quite similar to "coastal sage" in California, "tomilares" in Spain, and "batha" in Israel. Phrygana are low xeric and mostly spiny shrubs. They occupy areas towards the dry end of the precipitation gradient of the Mediterranean climate [46] and correspond to relatively heterogeneous fuel situations, usually including a variable percentage of phryganic species such as *Sarcopoterium spinosum*, *Phlomis fruticosa*, and *Cistus* spp. (*Cistus creticus*, *Cistus parviflorus*, *Cistus salvifolius*, and *Coridothymus capitatus*). They are pyrophytes, obligate seeders, and among the first shrubs to emerge after fire [47].

The current work had two main objectives. The first was to develop a fuel model for the most common species of *Cistus* in Greece (*Cistus creticus*, *Cistus parviflorus*, and *Cistus salvifolius*), also known by the common name of "rockroses", since they form a widespread vegetation type. They usually cover burned areas in the years immediately after a wildfire or occupy openings in low-altitude pine forests (e.g., Aleppo pine (*Pinus halepensis*) or Calabrian pine (*Pinus brutia*)).

A fuel model representing such a fuel type can be utilized to describe phryganic areas of relatively low height in Greece and probably other countries of southeastern Europe where *Cistus* spp. phryganic lands are abundant.

The second objective of the paper was to examine whether the developed model can be used reliably to predict fire behavior in *Cistus* spp. phryganic lands. Surface fire ROS field observations, obtained in wildfires or prescribed burns (ROSobs), in areas covered by *Cistus* spp. in Greece, were utilized to evaluate the degree of agreement of BehavePlus predictions (ROSpred) with observed fire behavior for the developed *Cistus* spp. fuel model, to introduce adjustments if needed, and ultimately to contribute towards better fire behavior prediction in the phryganic lands of Greece.

2. Materials and Methods

The methods described in [48,49] were utilized to develop the *Cistus* spp. fuel model. The work was based on destructive fuel sampling and took place on Zakynthos island, western Greece, in the month of July (Figure 1).

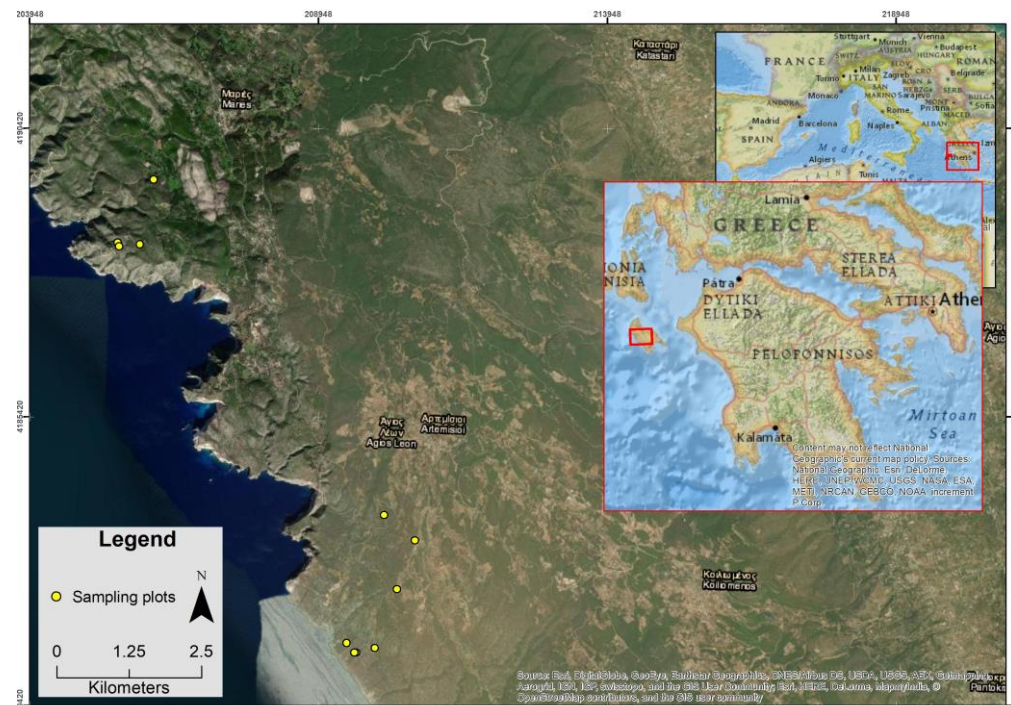


Figure 1. General area of the sampling plots in western Greece (Zakynthos island).

The sampling sites were selected based on discussions with local forest service officers followed by obtaining a record of the significant wildfires that had taken place on the island in the last five years. Such sites are covered by *Cistus* spp. immediately after the fires, which acts as a soil stabilizer and shade provider, helping the establishment and survival of other species such as pines. Thus, for the first post-fire years, the sites are occupied by *Cistus* spp. [50] with a coverage that often exceeds 80%. It is later reduced when other resprouting shrubs and pine seedlings grow and occupy the site. Following the leads and data from the forest service, extensive on-site visits to these recently burned areas across all of the western part of the island (Figure 1) offered a good overview of *Cistus* spp.-covered sites in terms of vegetation height, structure, and density. By visually assessing the relatively small existing differences, it was possible to select a series of representative *Cistus* spp. sites to cover all of this variation.

At each sampling site, visually assessed as homogeneously covered by *Cistus* spp., an initial representative point was selected. Aiming to avoid any bias due to the selection of this specific point, the exact location for destructive sampling was determined by carrying

out a draw to define an azimuth. The next step was to walk in the azimuth direction and place a 2 m pole 30 m from the initial point (at the end of the randomly positioned transect, traced by a measuring tape). A camera was then placed on a tripod 1.6 m tall, at the 24 m mark of the tape, looking towards the pole, and the sampling site was documented before the start of the destructive sampling (Figure 2a,b,d).

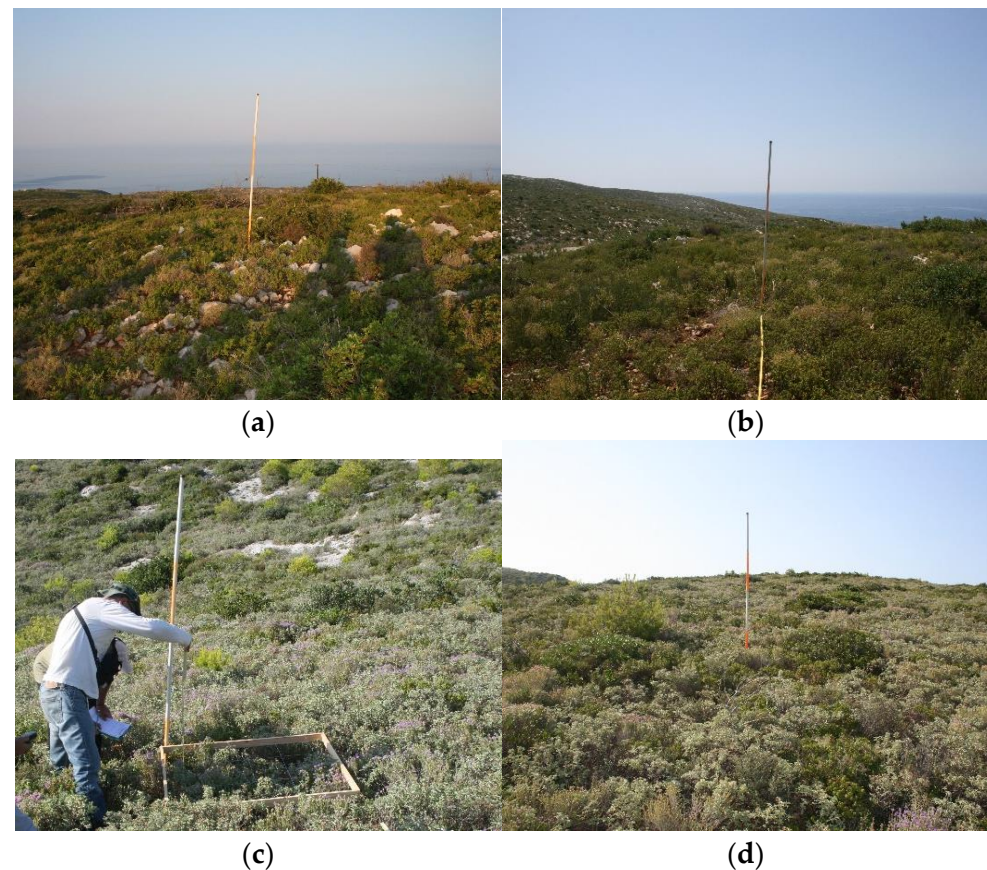


Figure 2. Sampling locations in phryganic sites covered by *Cistus* spp., where TFL: the average oven-dry total fuel loading ($\text{kg}\cdot\text{m}^{-2}$), SHRHGT: the average vegetation (shrub) height (cm), and SHRCOV: the vegetation cover (dimensionless) of the sampling location. The photographs are sorted by their SHRHGT value (lowest to highest). (a) TFL = 0.37, SHRHGT = 10, SHRCOV = 0.69, (b) TFL = 0.77, SHRHGT = 17, SHRCOV = 0.83, (c) TFL = 0.78, SHRHGT = 18, SHRCOV = 0.73, (d) TFL = 0.92, SHRHGT = 28, SHRCOV = 0.96.

Next, three plots, defined by 1×1 m wooden frames, were placed at 1 m intervals along the right side of the transect, starting at the 25 m mark (i.e., at 25–26, 27–28, and 29–30 m points). Within the 1 m^2 frames, there were five strings every 20 cm crossed by five perpendicular strings every 20 cm also, specifying 25 cross-points inside the frame. The vegetation height was measured at those 25 predetermined points within the plot (Figures 2c and 3a). A value of zero was noted when there was no vegetation under each of these 25 points. The average of the 25 measurements allowed the calculation of a mean height value for the plot (SHRHGT, cm).

The vegetation cover (SHRCOV, %) was calculated by dividing the number of non-zero values by 25 and multiplying by 100. For example, if there were five points where there was no shrub vegetation (i.e., with height values equal to zero), the SHRCOV of the plot was calculated as 80%. All live and dead fuels within the plots were cut, collected, and weighed to calculate fuel loading ($\text{kg}\cdot\text{m}^{-2}$) and to obtain information on the distribution of the live and dead fuels' size classes (Table 1) that is needed for fuel modeling (Table 2).

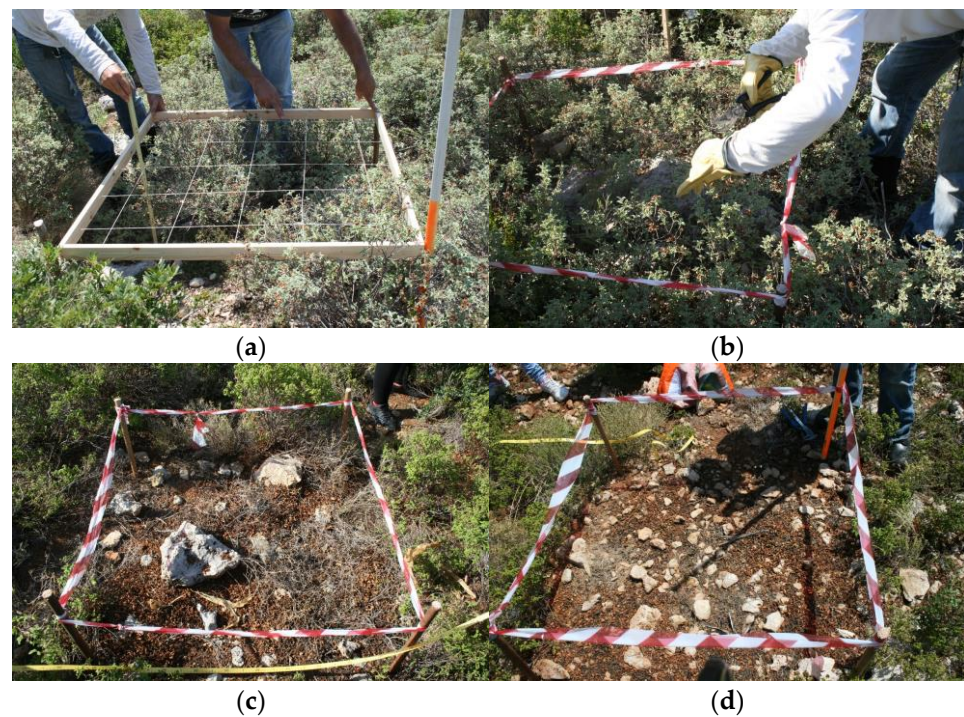


Figure 3. Stages of the destructive sampling process in sampling plots. (a) measuring vegetation height, (b) cutting and collecting live fuels, (c) dead fuels are to be collected, and weighed, (d) all live and dead fuels have been collected.

Table 1. Descriptive statistics for (a) total oven-dry fuel loading (TFL, $\text{kg}\cdot\text{m}^{-2}$) and oven-dry fuel loadings of the live and dead fuel classes ($\text{kg}\cdot\text{m}^{-2}$), (b) vegetation height (SHRHGT, cm), and (c) vegetation cover (SHRCOV, %) for $N = 30$ sampling plots.

Variable	Units	Mean	Median	Standard Deviation	Min	Max	N
TFL	$\text{kg}\cdot\text{m}^{-2}$	0.74	0.68	0.39	0.17	1.56	30
Live (up to 0.64 cm)	$\text{kg}\cdot\text{m}^{-2}$	0.27	0.25	0.16	0.05	0.79	30
Live (0.64 to 2.54 cm)	$\text{kg}\cdot\text{m}^{-2}$	0.04	0.02	0.05	0	0.18	30
Dead (1-hr)	$\text{kg}\cdot\text{m}^{-2}$	0.39	0.34	0.26	0.09	1.00	30
Dead (10-hr)	$\text{kg}\cdot\text{m}^{-2}$	0.04	0.02	0.05	0	0.20	29
SHRHGT	cm	21	21	8	6	37	30
SHRCOV	%	80	80	12	44	100	30

Table 2. Values of the parameters of the fuel model for *Cistus* spp.

Fuel Class	Fuel Load ($\text{tn}\cdot\text{ha}^{-1}$)	SA/V ($\text{cm}^2\cdot\text{cm}^{-3}$)	Other Parameters	Value
1-hr	3.95	23.46	Fuel bed depth (cm)	9.44
10-hr	0.38	3.57 (BEHAVE)	Fuel heat content ($\text{kJ}\cdot\text{kg}^{-1}$)	19.046
100-hr	0.01	0.98 (BEHAVE)	Moisture of extinction (%)	46
Live Herbaceous	0.00	-		
Live Woody	3.10	30.00		

By using a go/no-go gauge [48], the live and dead fuels were separated according to size (diameter) classes and their wet weight was weighed in situ with a portable electronic scale with a precision of 0.1 g. Regarding live fuels, the first class with a diameter up to 0.64 cm included foliage and twigs. A second class included twigs with a diameter from

0.64 to 2.54 cm. Due to the type of vegetation (*Cistus* spp.-dominated phryganic fields), there was no thicker live vegetation.

After the live fuel classes were removed from the plot, the dead fuels were also collected and weighed in size classes. The first class included the 1-hr time lag fuels (dead twigs with a diameter up to 0.64 cm, litter, and, in a few cases, dead grass). The second class included the 10-hr dead woody fuels with a diameter from 0.64 to 2.54 cm, and the third class included the 100-hr fuels with a diameter from 2.54 to 7.62 cm. This dead fuel class was only found in one plot and was a branch of *Phillyrea latifolia*.

The dead fuel size classes are used as moisture time lag standards in the US National Fire-Danger Rating System [51]. A moisture time lag is the length of time for a substance to lose or gain approximately two-thirds of the moisture above or below its equilibrium moisture [48].

Finally, the total oven-dry fuel loading (TFL, $\text{kg}\cdot\text{m}^{-2}$) was calculated by summing up the oven-dry fuel loadings of all fuel size classes. Twenty-one measurements of ROSobs made in the field (Table 3) during the evolution of wildfires [45] and prescribed burns [52], in areas covered by *Cistus* spp. in Greece, were utilized to evaluate the degree of agreement of BehavePlus predictions for the developed *Cistus* spp. fuel model with observed fire behavior.

Table 3. Descriptive statistics summary for measurements conducted in the field during wildfires and prescribed burns, namely, (a) ROSobs, (b) midflame wind speed (V_{midflame}), (c) fine dead (1-hr) and LW FMC, (d) and slope.

Variable	Units	Mean	Median	Standard Deviation	Standard Error	Min	Max	N
ROS _{obs}	$\text{m}\cdot\text{min}^{-1}$	2.6	1.3	3.4	0.8	0	12	21
V_{midflame}	$\text{km}\cdot\text{h}^{-1}$	6.1	5	8.5	1.8	0	30	21
1-hr FMC	%	14.7	10	8.7	1.9	7	42.1	21
LW FMC	%	75.2	31	47.7	10.4	31	128	21
Slope	%	36.4	36	32.5	7.1	0	100	21

Predictions of ROS for the *Cistus* spp. fuel model (ROSpred) were compared with ROS observations (ROSobs) in *Cistus* spp. dominated phryganic areas in Greece. These 21 fire behavior observations (ROSobs) were matched with the related meteorological, topography, and forest fuel information following specific procedures [3,10,52]. The ROSobs ($\text{m}\cdot\text{min}^{-1}$) were calculated by tracking wildfire perimeters and knowing the exact time for fire head, flank, or heel location and by using GIS software, using the following steps: The observer's positions were identified using a GPS device and the geographic coordinates were recorded. Regarding ground photography shooting, photographs of the sequential locations of the fire perimeter were taken using a Canon EOS 70D DSLR camera. For all shots, the horizontal azimuths were recorded using a compass.

Later, in the office, the fire perimeter (head, flank, or heel) locations were pinpointed on the map using the ArcGIS 9.3 Geographic Information System (GIS) software by ESRI. The time each photo was captured was identified from the data recorded automatically by the camera on the digital photo file that was in JPG format. By knowing the exact time for every fire perimeter location [1], the ROSobs values were calculated. Regarding prescribed burning ROSobs data, the recording of fire behavior additionally included aerial photographs that were taken from unmanned aerial vehicles (UAVs) [52]. We used a DJI Phantom 4 Pro, since it provides wind resistance up to 10 m/sec, more than 20 min of autonomous flight per battery, and carries an 1" CMOS, 20 Mp sensor, with FOV 84° 8.8 mm/24 mm (35 mm format equivalent) f/2.8–f/11 auto focus at 1 m–∞ lens and a mechanical/electronic shutter speed of 8–1/2000 sec. Images were created in JPEG format of 5472 × 3648 pixels.

3. Results

The number of sampling locations reached 10, so, with 3 plots per location, there were 30 sampling plots in total. According to the visual assessments in those 30 sampling plots, the phryganic areas were composed of 35% *Cistus creticus*, 29% *Cistus parviflorus*, 9% *Cistus salvifolius*, and 7% *Coridothymus capitatus*. The descriptive statistics of the dataset of 30 sampling plots regarding (a) total oven-dry fuel loading (TFL, $\text{kg}\cdot\text{m}^{-2}$) and oven-dry fuel loadings of the live and dead fuel classes, (b) vegetation height (SHRHGT, cm) and (c) vegetation cover (SHRCOV, %) are presented in Table 1.

As shown in Table 1, the sampling plots were in phryganic areas of relatively low vegetation height and varying cover. The mean and median values of SHRHGT were equal to 21 cm, while those of SHRCOV were equal to 80%. The variance of TFL was 0.155 and its mean value 0.74 kg m^{-2} , so for a maximum acceptable deviation equal to 20% of the mean value (0.148 kg m^{-2}) and a confidence level of 95%, the required sample size is $N = 27$, which is smaller than the actual number of sampling plots ($N = 30$).

The development of the *Cistus* spp. fuel model started by utilizing some important observations regarding the attributes of the fuel type. The fuel loading of the live fuels with a diameter from 0.64 to 2.54 cm was less than 15% of the total live fuel loading. As nearly all of this loading was quite fine, closer to 0.64 than to 2.54, as observed by using a go/no-go gauge during destructive sampling, it was added to the class of the live fuels with a diameter up to 0.64 cm. This class of live fuels is the “Live Woody” (LW) parameter of the fuel model. According to the field observations of the first author, in actual fires spreading through phryganic areas, the stems of *Cistus* spp. that are a little thicker than 0.64, as a rule, are completely consumed by the flames, contributing to the overall fire behavior, thus fully justifying the decision to include them in the LW category together with the finer live fuels. Omitting live fuel thicker than 0.64 cm, while it is clear that it is burned during the passage of the fire front, would result in an obvious underestimation of the true fuel loading.

Regarding the development of the fuel model, in addition to the measured parameters, it is necessary to determine a number of additional ones, namely, the surface area-to-volume ratio (SA/V, $\text{cm}^2\cdot\text{cm}^{-3}$) of 1-hr fuels, the SA/V of ‘Live Herbaceous’ vegetation and the SA/V of the LW, the fuel heat content ($\text{kJ}\cdot\text{kg}^{-1}$), the fuel bed depth (cm), and the moisture of extinction (%) which is the moisture content value of the dead fuels at which the fire stops spreading [36].

For LW fuels SA/V, the value of $30 \text{ cm}^2\cdot\text{cm}^{-3}$ was adopted as an approximate weighted average of the value of $44.49 \text{ cm}^2\cdot\text{cm}^{-3}$ measured by Dimitrakopoulos [43] for *Cistus salvifolius* leaves, $23.01 \text{ cm}^2\cdot\text{cm}^{-3}$ for live twigs with a diameter less than 0.64 cm diameter, and $8.09 \text{ cm}^2\cdot\text{cm}^{-3}$ for live twigs with a diameter from 0.64 to 2.54 cm.

Live fine herbaceous vegetation was not found during the destructive sampling; therefore, an SA/V value was not specified for that parameter. For fine dead (1-hr) fuels, the value of $23.46 \text{ cm}^2\cdot\text{cm}^{-3}$ measured by [43] for thin dead twigs of *Cistus salvifolius* was adopted. For the fuel heat content, the value of 19.046 kJ/kg reported by [43] for *Cistus salvifolius* was adopted.

The above-mentioned data were processed through the NEWMDL subsystem of BEHAVE [36] to develop the *Cistus* spp. fuel model. Moreover, a weighted value for the fuel bed depth and a value for the moisture of extinction, which is very difficult to measure in practice, were then calculated. Typical photos of *Cistus* spp.-dominated phryganic fields of various height and cover are shown in Figure 2 and the values of the *Cistus* spp. fuel model’s parameters are presented in Table 2. They include values of SA/V for the 10-hr and 100-hr fuels adopted by default by BEHAVE [36].

Twenty-one measurements of ROSobs made in the field (Table 3) during the evolution of wildfires and prescribed burns, in areas covered by *Cistus* spp. in Greece, were utilized to evaluate the degree of agreement of BehavePlus predictions for the *Cistus* spp. fuel model with the observed fire behavior. The *Cistus* spp. fuel model (Table 2) and measurements of the dead and live woody fuels’ moisture content (FMC), slope, and midflame wind-

speed (Table 3) were used as input for predicting the surface fire rate of spread (ROSpred, $\text{m}\cdot\text{min}^{-1}$) values with BehavePlus.

The pairs of ROSobs and ROSpred values were correlated via linear regression, resulting in Equation (1), with an adjusted $R^2 = 0.879$. The plot of Equation (1), including the 95% confidence interval (blue dotted lines), is shown in Figure 4.

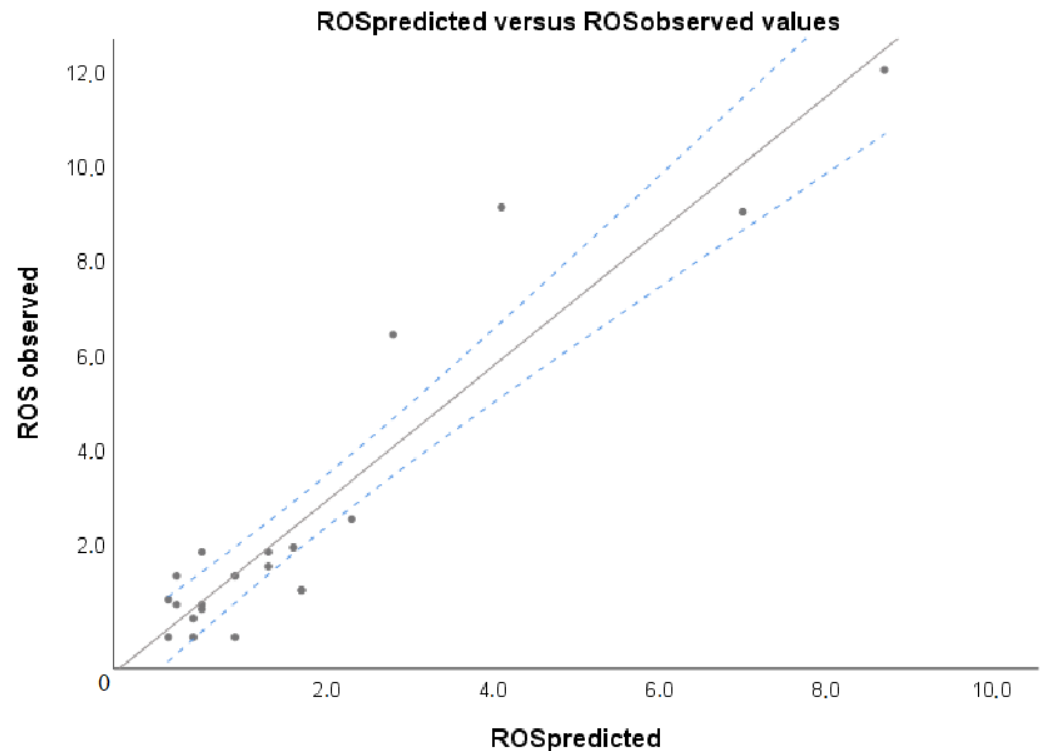


Figure 4. Linear regression between ROSobs and ROSpred values ($\text{m}\cdot\text{min}^{-1}$) for the *Cistus* spp. fuel model, including the 95% confidence interval.

$$\text{ROSobs} = 0.037 + 1.425 \cdot \text{ROSpred}, \quad (1)$$

Equation (1) is statistically significant ($p < 0.001$). The 95% confidence interval for the regression is [1.12, 4.00]. The p -value of the slope coefficient is also statistically significant ($p < 0.001$) and its 95% confidence interval is [1.179, 1.672]. The p -value of the constant of Equation (1) is not statistically significant (p -value = 0.914). The adjusted R^2 value of the regression of Equation (1) indicates that its unexplained error is relatively low.

4. Discussion

The regression equation for the prediction of ROSobs values from BehavePlus ROSpred values is statistically significant and has a good adjusted R^2 value. The value of the slope coefficient is equal to 1.425. The fact that the 95% confidence interval is 1.179 to 1.672, and does not include the value of 1, means that the BehavePlus ROSpred under-predicts the actual rate of spread. This under-prediction should be taken into consideration when using BehavePlus with the *Cistus* spp. fuel model for ROS prediction in phryganic areas.

On the other hand, the constant of the equation is not statistically significant ($p = 0.914$). This means that the intercept can be considered equal to zero. However, in the statistical interpretation, the value of the intercept of $0.037 \text{ m}\cdot\text{min}^{-1}$ is almost equal to 0, and Equation (1) can be used for all practical purposes. This is also evident in Figure 4.

Four observations at the upper end of the ROS values in Figure 4 seem to influence the slope of the regression equation. Regarding their influence and leverage, we could mention that point 6 (ROSpred = 8.7, ROSobs = 12.0) seems to be of high leverage, but of relatively low influence, as does point 4 (7.0, 9.0) (see Figures 5 and 6). As for point 10 (4.1, 9.1), it

seems to be of low leverage and of relatively high influence, which does not seem to be the case for point 9 (2.8, 6.4). By removing point 10, which is the point with the maximum Cook's distance (0.446) [53], the regression does not change substantially and the adjusted R^2 is improved (from 0.879 to 0.913). The point can be marginally considered a potential outlier since the Cook's distance does not exceed 0.5.

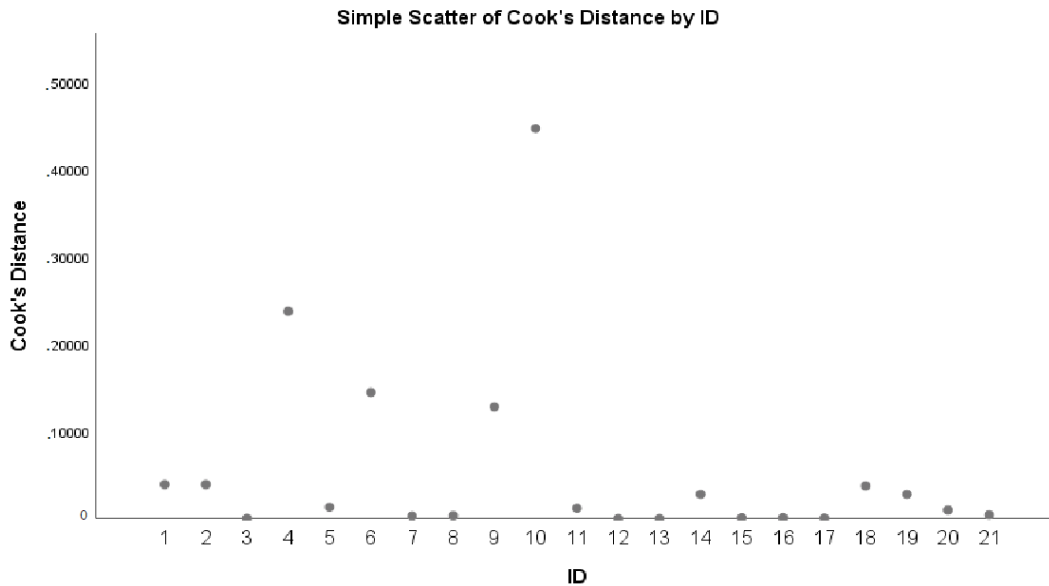


Figure 5. Cook's distance values for the 21 data points of Figure 4.

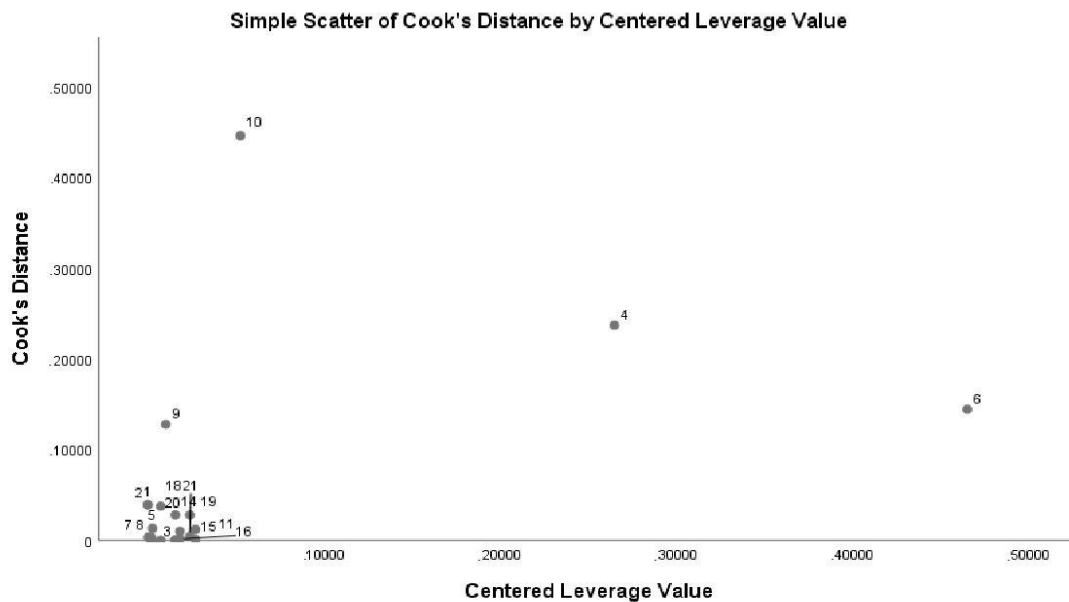


Figure 6. Centered leverage versus Cook's distance values for the 21 data points of Figure 4.

Table 4 shows the calculated ROSpred ($m \cdot min^{-1}$) values with BehavePlus using the *Cistus* spp. fuel model, setting the 1-hr and 10-hr fuel moisture content (FMC) at 5%, 100-hr fuel FMC at 7%, and LW FMC at 80%, and examining the influence of midflame wind ($km \cdot hr^{-1}$) and slope (%) on the predictions. It also shows, in parenthesis, the corresponding expected ROSobs values obtained through Equation (1).

Table 4. ROS predictions (ROSpred, $\text{m}\cdot\text{min}^{-1}$) for a range of midflame wind speed and slope conditions in *Cistus* spp. phryganic fields. The corresponding solutions of Equation (1) in parentheses stand for the corresponding expected ROSobs values.

Midflame Wind Speed, $\text{km}\cdot\text{h}^{-1}$	Slope Steepness (%)				
	0 (Horizontal)	10	30	60	100
0	0.1 (0.2)	0.1 (0.2)	0.3 (0.5)	0.8 (1.2)	2.0 (2.9)
1.1	0.3 (0.5)	0.3 (0.5)	0.4 (0.6)	1.0 (1.5)	2.2 (3.2)
2.8	0.5 (0.7)	0.5 (0.7)	0.7 (1.0)	1.2 (1.7)	2.4 (3.5)
5	0.8 (1.2)	0.8 (1.2)	1.0 (1.5)	1.5 (2.2)	2.7 (3.9)
7.7	1.2 (1.7)	1.2 (1.7)	1.3 (1.9)	1.8 (2.6)	3.0 (4.3)

The ROS underprediction when using BehavePlus with the *Cistus* spp. fuel model was given further thought in an effort to explain the discrepancy. The careful observation of photos of the fuel conditions during the fires in which the ROS observations were made revealed that there was a varying presence and mix of grass, mainly *Brachypodium ramosum*, in various growth stages. In the summer fires, there was no presence of this grass, while in winter-prescribed burns, there was a significant contribution of *Brachypodium ramosum* loading with a moisture content exceeding 40% (Table 3). The occurrence of this grass affected the fire behavior in winter, accelerating the fire spread, and is partially responsible for the fire spread observations that are higher than those obtained using BehavePlus with the *Cistus* spp. fuel model. The fuel model was based on summer measurements without the presence of *Brachypodium ramosum*.

The maximum and mean vegetation height (SHRHGT) in the sampling plots were 37 and 21 cm, respectively (Table 1), but the fuel bed depth of the *Cistus* spp. fuel model was 9.44 cm (Table 2). This can be explained by the fact that the vegetation across those phryganic areas is sparse with many gaps where SHRHGT is equal to 0. Thus, the mean weighted fuel depth is quite low, even though the height of *Cistus* spp. shrublands visually appears taller than 10 cm (Figures 2c,d, 3a,b and 4a). SHRCOV varied from 44 to 100%, while its mean and median values were equal to 80% (Table 1).

Regarding fire behavior observations, in calm and wet conditions such as those encountered in the prescribed burns, the fire spread slowly with low intensity and eventually stopped when it reached less dense vegetation. In three cases, it was observed that in calm conditions ($V_{\text{midflame}} = 0$) and slopes varying from 60 to 84%, the fire stopped spreading ($R_{\text{obs}} = 0 \text{ m}\cdot\text{min}^{-1}$) through the *Cistus* spp.-dominated phryganic areas with 1-hr FMC equal to 20 or 42% and LW FMC equal to 128%. For those cases, the ROS predictions (R_{pred}), which refer to the fire spread through a homogeneous and continuous fuel bed, were different than zero, varying from 0.1 to $0.9 \text{ m}\cdot\text{min}^{-1}$. This is an indication that the moisture of extinction of 46% calculated through BEHAVE and reported in Table 2 is probably higher than the observed one.

By examining Tables 1 and 2, it becomes evident that the fuel model for *Cistus* spp. can be utilized to describe phryganic areas of relatively low height (9 to 21 cm) and vegetation cover around 70%. The fuel situations in phryganic areas dominated by *Cistus creticus*, *Cistus parviflorus*, and *Cistus salvifolius* are found in southeastern Europe where grazing is also a factor that shapes the landscapes. The areas where destructive sampling took place (Figure 1) have burned more than two times in the last four decades. Over the last 38 years, several fires occurred at the same places of the island of Zakynthos, a pattern that is usually observed in areas with livestock grazing [54,55]. Figure 2a,b represent grazed, sparse, and low *Cistus* spp.-dominated phryganic lands.

The total oven-dry fuel loading of the *Cistus* spp. fuel model is $7.44 \text{ tn}\cdot\text{ha}^{-1}$, of which 58% is dead fuel. This value lies between the corresponding total fuel loading values of two published fuel models of Dimitrakopoulos [43,44,56] for phryganic vegetation in Greece, namely, the models for *Sarcopoterium spinosum* and for *Phlomis fruticosa*. The total oven-dry fuel loading of the former is $5.65 \text{ tn}\cdot\text{ha}^{-1}$, of which 85% is dead fuel. The total oven-dry fuel loading of the latter is $9.9 \text{ tn}\cdot\text{ha}^{-1}$, of which 74% is dead fuel. These differences are

large enough and affect fire behavior substantially, justifying the development of the *Cistus* spp. model that lies, in terms of total fuel loading, between the two.

Finally, it should also be pointed out that the *Cistus* spp. fuel model for Greece is quite likely not appropriate for other areas of the Mediterranean such as the Iberian Peninsula. The *Cistus* species there, according to the published literature, are generally taller and the corresponding fuel loading should be expected to be much higher. Examples are *Cistus ladanifer* (height = 115 ± 32.4 cm) [57], *Cistus laurifolius* L. (average height = 98.2 ± 3 cm) [58], and *Cistus albidus* L. (height up to 150 cm) [47].

5. Conclusions

The finding that BehavePlus underpredicts the actual rate of fire spread should be taken into consideration when using the system with the *Cistus* spp. fuel model for ROS prediction in phryganic areas. Adjusting the rate of fire spread predictions by utilizing Equation (1) and its 1.4 adjustment factor is one way to apply this information in the field, especially during the fire season. More fire behavior observations in the future, during prescribed fires and wildfires of higher intensity, will help to identify possible overpredictions or underpredictions, especially for environmental parameter values outside the range already tested, and to evaluate the overall reliability of the proposed equation.

Author Contributions: Conceptualization, M.A.; methodology, M.A. and A.M.; formal analysis, M.A. and E.K.; resources, M.A. and E.V.A.; writing—original draft preparation, M.A.; writing—review and editing, M.A., A.M., E.K. and E.V.A.; visualization, M.A.; supervision, M.A. All authors have read and agreed to the published version of the manuscript.

Funding: This research received no external funding.

Institutional Review Board Statement: Not applicable.

Informed Consent Statement: Not applicable.

Data Availability Statement: Data are available upon request.

Acknowledgments: We would like to thank the students of the Department of Environment of Ionian University, who helped us during destructive samplings in the field and in the laboratory.

Conflicts of Interest: The authors declare no conflict of interest.

References

- Alexander, M.E.; Cruz, M. Fireline Intensity. In *Encyclopedia of Wildfires and Wildland-Urban Interface (WUI) Fires*; Springer: Berlin/Heidelberg, Germany, 2019; pp. 1–8.
- Davis, K.P. *Forest Fire, Control and Use*; McGraw-Hill Book Co., Inc.: New York, NY, USA, 1959; p. 584.
- Athanasiou, M.; Xanthopoulos, G. Fire Behaviour of the Large Fires of 2007 in Greece. In Proceedings of the 6th International Conference on Forest Fire Research, Coimbra, Portugal, 15–18 November 2010.
- Rothermel, R.C. *A Mathematical Model for Predicting Fire Spread in Wildland Fuels*, R.P. INT-115 ed.; Department of Agriculture, Intermountain Forest and Range Experiment Station: Ogden, UT, USA, 1972; p. 40.
- Salis, M.; Arca, B.; Alcasena, F.; Arianoutsou, M.; Bacciu, V.; Duce, P.; Duguy, B.; Koutsias, N.; Mallinis, G.; Mitsopoulos, I. Predicting wildfire spread and behaviour in Mediterranean landscapes. *Int. J. Wildland Fire* **2016**, *25*, 1015–1032. [[CrossRef](#)]
- Andrews, P.L. *The Rothermel Surface Fire Spread Model and Associated Developments: A Comprehensive Explanation*; General Technical Report RMRS-GTR-371; Department of Agriculture, Forest Service, Rocky Mountain Research Station: Fort Collins, CO, USA, 2018; p. 121.
- McAlpine, R.; Xanthopoulos, G. Predicted vs. Observed fire spread rates in ponderosa pine fuel beds: A test of American and Canadian systems. In Proceedings of the 10th Conference on Fire and Forest Whitewood Compte rendu du 10ieme Congress sur les incendies et la meteorologie forestiere, Ottawa, ON, Canada, 17–21 April 1989; Maiver, D., Auld, H., Whitewoo, R., Eds.; Ottawa, Ont. Forestry Canada: Ottawa, ON, Canada, 1989; pp. 287–294.
- Van Wilgen, B.W.; Le Maitre, D.C.; Kruger, F.J. Fire Behaviour in South African Fynbos (Macchia) Vegetation and Predictions from Rothermel's Fire Model. *J. Appl. Ecol.* **1985**, *22*, 207. [[CrossRef](#)]
- Xanthopoulos, G. *A Fuel Model for Fire Behavior Prediction in Spotted Knapweed (Centaurea maculosa L.) Grasslands in Western Montana*; The University of Montana: Missoula, MT, USA, 1986.

10. Athanasiou, M.; Xanthopoulos, G. Wildfires in Mediterranean shrubs and grasslands. In Greece: In situ fire behaviour observations versus predictions. In Proceedings of the 7th International Conference on Forest Fire Research on Advances in Forest Fire Research, Coimbra, Portugal, 17–20 November 2014.
11. Drury, S.A. Observed versus predicted fire behavior in an Alaskan black spruce forest ecosystem: An experimental fire case study. *Fire Ecol.* **2019**, *15*, 35. [[CrossRef](#)]
12. Andrews, P.L.; Bevins, C.; Seli, R. *BehavePlus Fire Modeling System, Version 4.0: User's Guide*; General Technical Report RMRS-GTR-106 Revised; Department of Agriculture, Forest Service, Rocky Mountain Research Station: Ogden, UT, USA, 2005; Volume 106, p. 132.
13. Andrews, P.L. Current status and future needs of the BehavePlus Fire Modeling System. *Int. J. Wildland Fire* **2014**, *23*, 21–33. [[CrossRef](#)]
14. Papadopoulos, G.D.; FPavlidou, N. A comparative review on wildfire simulators. *IEEE Syst. J.* **2011**, *5*, 233–243. [[CrossRef](#)]
15. Finney, M.A. Modeling the spread and behavior of prescribed natural fires. In Proceedings of the 12th Conference Fire and Forest Meteorology, Jekyll Island, GA, USA, 26–28 October 1994.
16. Finney, M.A. *FARSITE, Fire Area Simulator—Model Development and Evaluation*; US Department of Agriculture, Forest Service, Rocky Mountain Research Station: Fort Collins, CO, USA, 1998.
17. Finney, M.A. An Overview of FlamMap Fire Modeling Capabilities. In *Fuels Management—How to Measure Success: Conference Proceedings*; USDA Forest Service, Rocky Mountain Research Station: Fort Collins, CO, USA, 2006.
18. Andrews, P.L.; Cruz, M.; Rothermel, R. Examination of the wind speed limit function in the Rothermel surface fire spread model. *Int. J. Wildland Fire* **2013**, *22*, 959–969. [[CrossRef](#)]
19. Sullivan, A.L. Wildland surface fire spread modelling, 1990–2007, 2: Empirical and quasi-empirical models. *Int. J. Wildland Fire* **2009**, *18*, 369–386. [[CrossRef](#)]
20. Cruz, M.G.; Alexander, M.E. The 10% wind speed rule of thumb for estimating a wildfire's forward rate of spread in forests and shrublands. *Ann. For. Sci.* **2019**, *76*, 44. [[CrossRef](#)]
21. Cruz, M.G.; Alexander, M.E.; Fernandes, P.M.; Kilinc, M.; Sil, Â. Evaluating the 10% wind speed rule of thumb for estimating a wildfire's forward rate of spread against an extensive independent set of observations. *Environ. Model. Softw.* **2020**, *133*, 104818. [[CrossRef](#)]
22. Fernandes, P.A.M. Fire spread prediction in shrub fuels in Portugal. *For. Ecol. Manag.* **2001**, *144*, 67–74. [[CrossRef](#)]
23. Bilgili, E.; Saglam, B. Fire behavior in maquis fuels in Turkey. *For. Ecol. Manag.* **2003**, *184*, 201–207. [[CrossRef](#)]
24. Saglam, B.; Bilgili, E.; Küçük, Ö.; Durmaz, B.D. Fire behavior in Mediterranean shrub species (Maquis). *Afr. J. Biotechnol.* **2008**, *7*, 4122–4129.
25. Sullivan, A.L. Wildland surface fire spread modelling, 1990–2007. 1: Physical and quasi-physical models. *Int. J. Wildland Fire* **2009**, *18*, 349–368. [[CrossRef](#)]
26. Sullivan, A.L. Wildland surface fire spread modelling, 1990–2007. 3: Simulation and mathematical analogue models. *Int. J. Wildland Fire* **2009**, *18*, 387–403. [[CrossRef](#)]
27. Koo, E.; Pagni, P.; Stephens, S.; Huff, J.; Woycheese, J.; Weise, D. A Simple Physical Model For Forest Fire Spread Rate. *Fire Saf. Sci.* **2005**, *8*, 851–862. [[CrossRef](#)]
28. Zhou, X.; Mahalingam, S.; Weise, D. Modeling of marginal burning state of fire spread in live chaparral shrub fuel bed. *Combust. Flame* **2005**, *143*, 183–198. [[CrossRef](#)]
29. Balbi, J.-H.; Morandini, F.; Silvani, X.; Filippi, J.-B.; Rinieri, F. A physical model for wildland fires. *Combust. Flame* **2009**, *156*, 2217–2230. [[CrossRef](#)]
30. Linn, R.; Reisner, J.; Colman, J.J.; Winterkamp, J. Studying wildfire behavior using FIRETEC. *Int. J. Wildland Fire* **2002**, *11*, 233–246. [[CrossRef](#)]
31. Coen, J.L. *Modeling Wildland Fires: A Description of the Coupled Atmosphere Wildland Fire Environment Model (CAWFE)*; NCAR Technical Notes; NCAR: Boulder, CO, USA, 2013.
32. Coen, J.L.; Cameron, M.; Michalakes, J.; Patton, E.; Riggan, P.J.; Yedinak, K.M. WRF-Fire: Coupled Weather–Wildland Fire Modeling with the Weather Research and Forecasting Model. *J. Appl. Meteorol. Clim.* **2013**, *52*, 16–38. [[CrossRef](#)]
33. Mandel, J.; Beezley, J.D.; Kochanski, A.K. Coupled atmosphere-wildland fire modeling with WRF 3.3 and SFIRE 2011. *Geosci. Model Dev.* **2011**, *4*, 591–610. [[CrossRef](#)]
34. Baptiste Filippi, J.; Bosseur, F.; Mari, C.; Lac, C.; Le Moigne, P.; Cuenot, B.; Veynante, D.; Cariolle, D.; Balbi, J.H. Coupled atmosphere-wildland fire modelling. *J. Adv. Model. Earth Syst.* **2009**, *1*, 11. [[CrossRef](#)]
35. Thomas, C.M.; Sharples, J.J.; Evans, J.P. Modelling the dynamic behaviour of junction fires with a coupled atmosphere–fire model. *Int. J. Wildland Fire* **2017**, *26*, 331. [[CrossRef](#)]
36. Burgan, R.E.; Rothermel, R.C. *BEHAVE: Fire Behavior Prediction and Fuel Modeling System—FUEL Subsystem*; General Technical Report INT-167; US Department of Agriculture, Forest Service, Intermountain Forest and Range Experiment Station: Ogden, UT, USA, 1984; Volume 167, p. 126.
37. Anderson, H.E. *Aids to Determining Fuel Models for Estimating Fire Behavior*; General Technical Report INT-GTR-122; U.S. Department of Agriculture, Forest Service, Intermountain Forest and Range Experiment Station: Rocky Mountain Research Station: Ogden, UT, USA, 1982.

38. Baughman, R.G.; Albini, F. Estimating midflame windspeeds. In Proceedings of the Sixth Conference on Fire and Forest Meteorology, Seattle, WA, USA, 22–24 April 1980.
39. Andrews, P.L. *Modeling Wind Adjustment Factor and Midflame Wind Speed for Rothermel's Surface Fire Spread Model*; General Technical Report RMRS-GTR-266; US Department of Agriculture, Forest Service, Rocky Mountain Research Station: Fort Collins, CO, USA, 2012; Volume 266, p. 39.
40. Fischer, W.C. *Wilderness Fire Management Planning Guide*; General Technical Report INT-GTR-171; U.S. Department of Agriculture, Forest Service, Intermountain Forest and Range Experiment Station: Ogden, UT, USA, 1984; Volume 56.
41. Turner, J.A.; Lawson, B. *Weather in the Canadian Forest Fire Danger Rating System: A User Guide to National Standards and Practices*; Information Report BC-X-1771978; Canadian Forest Service, Pacific Forestry Centre: Victoria, BC, Canada, 1984; p. 40.
42. Lawson, B.; Armitage, O. *Weather Guide for the Canadian Forest Fire Danger Rating System. A User Guide to National Standards and Practices*; Information Report BC-X-177; Fisheries and Environment Canada, Canadian Forest Service, Pacific Forest Research Centre: Victoria, BC, Canada, 2008; p. 40.
43. Dimitrakopoulos, A.; Panov, P. Pyric properties of some dominant Mediterranean vegetation species. *Int. J. Wildland Fire* **2001**, *10*, 23–27. [[CrossRef](#)]
44. Dimitrakopoulos, A. Mediterranean fuel models and potential fire behaviour in Greece. *Int. J. Wildland Fire* **2002**, *11*, 127–130. [[CrossRef](#)]
45. Athanasiou, M. Development of an Optimal Methodology for Forecasting Forest Fire Behaviour in Greece. In *Department of Geology and Geoenvironment*; National and Kapodistrian University of Athens: Athens, Greece, 2015; p. 408.
46. Sgardelis, S.; Pantis, J.; Argyropoulou, G.; Stamou, G. Effects of fire on soil macroinvertebrates in a Mediterranean phryganic ecosystem. *Int. J. Wildland Fire* **1995**, *5*, 113–121. [[CrossRef](#)]
47. Palá-Paúl, J.; Velasco-Negueruela, A.; Pérez-Alonso, M.J.; Sanz, J. Seasonal variation in chemical composition of *Cistus albidus* L. from Spain. *J. Essent. Oil Res.* **2005**, *17*, 19–22. [[CrossRef](#)]
48. Brown, J. *Handbook for Inventorying Downed Woody Material*; General Technical Report INT-16; Department of Agriculture, Forest Service, Intermountain Forest and Range Experiment Station: Ogden, UT, USA, 1974.
49. Xanthopoulos, G.; Manasi, M. A Practical Methodology for the Development of Shrub Fuel Models for Fire Behavior Prediction. In Proceedings of the IV International Conference on Forest Fire Research 2002, Wildland Fire Safety Summit, Luso, Coimbra, Portugal, 18–23 November 2002.
50. Arianoutsou, M. Aspects of demography in post-fire Mediterranean plant communities of Greece. In *Landscape Disturbance and Biodiversity in Mediterranean-Type Ecosystems*; Rundel, P., Montenegro, G., Jaksic, F.M., Eds.; Springer: New York, NY, USA, 1998; pp. 273–295.
51. Deeming, J.E.; Burgan, R.; Cohen, J. *The National Fire-Danger Rating System—1978, 1977*, United States Department of Agriculture, Forest Service, General Technical Report INT-39; Intermountain Forest and Range Experiment Station: Ogden, UT, USA, 1977; p. 66.
52. Athanasiou, M.; Bouchounas, T.; Korakaki, E.; Tziritis, E.; Xanthopoulos, G.; Sitara, S. Introducing the use of fire for wildfire prevention in Greece: Pilot application of prescribed burning in Chios island. In Proceedings of the 9th International Conference on Forest Fire Research: Advances in Forest Fire Research & 17th International Wildland Fire Safety Summit, Coimbra, Portugal, 11–18 November 2022.
53. Cook, R.D. Detection of influential observation in linear regression. *Technometrics* **1977**, *19*, 15–18.
54. Blondel, J.; Aronson, J.; Bodiou, J.Y.; Boeuf, G. *The Mediterranean Region: Biological Diversity in Space and Time*; Oxford University Press: Oxford, UK, 2010.
55. Kefalas, G.; Poirazidis, K.; Xofis, P.; Kalogirou, S. Mapping and Understanding the Dynamics of Landscape Changes on Heterogeneous Mediterranean Islands with the Use of OBIA: The Case of Ionian Region, Greece. *Sustainability* **2018**, *10*, 2986. [[CrossRef](#)]
56. Dimitrakopoulos, A.; Mateeva, V.; Xanthopoulos, G. Fuel models for Mediterranean vegetation types in Greece. *Geotech. Sci. Issues* **2001**, *12*, 192–206.
57. Carrión-Prieto, P.; Martín-Ramos, P.; Hernández-Navarro, S.; Sánchez-Sastre, L.F.; Marcos-Robles, J.L.; Martín-Gil, J. Valorization of *Cistus ladanifer* and *Erica arborea* shrubs for fuel: Wood and bark thermal characterization. *Maderas. Cienc. Y Tecnol.* **2017**, *19*, 443–454. [[CrossRef](#)]
58. Bados, R.; Esteban, L.S.; Esteban, J.; Fernández-Landa, A.; Sánchez, T.; Tolosana, E. Biomass equations for rockrose (*Cistus laurifolius* L.) shrublands in North-central Spain. *For. Syst.* **2021**, *30*, e015. [[CrossRef](#)]

Disclaimer/Publisher's Note: The statements, opinions and data contained in all publications are solely those of the individual author(s) and contributor(s) and not of MDPI and/or the editor(s). MDPI and/or the editor(s) disclaim responsibility for any injury to people or property resulting from any ideas, methods, instructions or products referred to in the content.